Synthetic and Systems Biotechnology 5 (2020) 316–323

Contents lists available at ScienceDirect

Synthetic and Systems Biotechnology

journal homepage: http://www.keaipublishing.com/synbio

Enhancing single-cell hyaluronic acid biosynthesis by microbial morphology engineering☆,

Yukun Zheng[a,b,1], Fangyu Cheng[a,b,1], Bo Zheng[a,b], Huimin Yu[a,b,c,*]

[a] Key Laboratory of Industrial Biocatalysis, Ministry of Education, Beijing, 100084, PR China
[b] Department of Chemical Engineering, Tsinghua University, Beijing, 100084, PR China
[c] Center for Synthetic and Systems Biology, Tsinghua University, Beijing, 100084, PR China

ARTICLE INFO

Keywords:
Morphology engineering
Single-cell HA-Producing capacity
DivIVA protein
FtsZ protein
Down/up dual regulation
Enlarged cells

ABSTRACT

Microbial morphology engineering is a novel approach for cell factory to improve the titer of target product in bio-manufacture. Hyaluronic acid (HA), a valuable glycosaminoglycan polymerized by HA synthase (HAS), a membrane protein, is particularly selected as the model product to improve its single-cell HA-producing capacity via morphology engineering. DivIVA and FtsZ, the cell-elongation and cell division related protein, respectively, were both down/up dual regulated in *C. glutamicum* via weak promoter substitution or plasmid overexpression. Different from the natural short-rod shape, varied morphologies of engineered cells, i.e. small-ellipsoid-like (DivIVA-reduced), bulb-like (DivIVA-enhanced), long-rod (FtsZ-reduced) and dumbbell-like (FtsZ-enhanced), were observed. Applying these morphology-changed cells as hosts for HA production, the reduced expression of both DivIVA and FtsZ seriously inhibited normal cell growth; meanwhile, overexpression of DivIVA didn't show morphology changes, but overexpression of FtsZ surprisingly change the cell-shape into long and thick rod with remarkably enlarged single-cell surface area (more than 5.2-fold-increase). And finally, the single-cell HA-producing capacity of the FtsZ-overexpressed *C. glutamicum* was immensely improved by 13.5-folds. Flow cytometry analyses verified that the single-cell HAS amount on membrane was enhanced by 2.1 folds. This work is pretty valuable for high titer synthesis of diverse metabolic products with microbial cell factory.

1. Introduction

In biotechnology and bioengineering, the yield of microbial bio-products can be increased by several ways such as metabolic engineering, enzyme engineering and process optimization. Besides these classic strategies, morphology engineering that regulating the genes in maintaining the cellular shapes of the bacteria becomes a novel approach to improve bio-manufacture. These cellular-shape-related target genes are also involved in cell growth, cell elongation or cell division [1], therefore cell morphology engineering can conversely be regulated by the processes of cell division and cell elongation [2]. Through morphology engineering, the bacterial cell-shapes can be shifted as expected from such as fibers to spheres, or small to large. These morphology changes subsequently influence the synthesis of target products [3,4], as well as cell growth, inclusion body accumulation and separation of products [5].

One of the most successful examples of cell morphology engineering in industrial biotechnology is the production of polyhydroxyalkanoate (PHA), an important polyester material accumulated as non-dissolved solid particles in the inner space of microorganism cells. The volume of bacterial cells is one of the limiting factors for PHA synthesis in host. Researchers therefore proposed different genetic strategies, i.e., inhibiting the expression of the cell-elongation-relevant cytoskeleton protein MreB and cell-division-relevant protein FtsZ, to achieve the changes in cell shape and cell volume in both *E. coli* and *halomonas* [5]. Through MreB regulation, the cells were rods in the early stage, then became spherical in later; at the same time, the cell volume increased correspondingly, and the intracellular PHA titer enhanced to 8.11 g/L from previous 4.44 g/L [1]. Through FtsZ inhibition (that is. The cell division ring is blocked), the shapes of the engineered cells changed from rods to fibers; meanwhile the titer of PHA products increased to 10.67 g/L. And also, the elongated cells can be precipitated naturally,

☆ Manuscript prepared for submission to:Synthetic and Systems Biotechnology.
Peer review under responsibility of KeAi Communications Co., Ltd.

* Corresponding author. Key Laboratory of Industrial Biocatalysis, Ministry of Education, Beijing 100084, PR China.
E-mail address: yuhm@mail.tsinghua.edu.cn (H. Yu).

[1] These two authors contributed equally to this work.

https://doi.org/10.1016/j.synbio.2020.09.002
Received 28 June 2020; Received in revised form 31 August 2020; Accepted 9 September 2020

thereby the cell harvesting process (e. g. centrifugation) can be simplified and the separation cost can be reduced [1,4].

Hyaluronic acid (HA) is a glycosaminoglycan used in many industries such as food, cosmetics and clinical medicine [6]. The hyaluronic acid synthase (HAS) is a membrane-binding protein, responsible for both HA polymerization and translocation [7]. *Streptococcus equi* is the natural HA-producing strain as industrial microorganisms at present [8]. After mutation breeding and cultivation process optimization, HA was produced in a 100 L fermentation tank with a yield of 6–7 g/L and a molecular weight of 3.2 MDa [9]. Recently, heterologous biosynthesis of HA was achieved in the engineered *E. coli*, *Bacillus subtilis*, *Lactococcus lactis* and *Corynebacterium glutamicum* [10–13]. Unlike *streptococcus*, *C. glutamicum* is a Generally-Recognized-*as*-Safe (GRAS) strain widely used in the food industry [14]. By introducing the HAS genes and optimizing the metabolic pathways, the high titer production of HA (28.7 g/L, 210kD Mw) was achieved in a 5 L fermentor with the engineered *C. glutamicum* ATCC13032 [15]. Further by introducing into the hyaluronidase, 74 g/L small 54kD Mw HA was also obtained [16].

The available membrane surface area can significantly influence the folding and yield of a membrane protein [17]. Considering that HAS is a membrane binding protein and the surface area of cell membrane would affect the HA synthesis capacity of single cell [18], the genes related to the cell morphology of *C. glutamicum* might be regulated to change the cell membrane amount, so as to enhance the HAS expression and single-cell HA synthesis capacity. Different from *E. coli* [3], DivIVA is another essential protein for cell elongation in *C. glutamicum*. The DivIVA oligomers are located at the two poles of cell and provide scaffolds for the peptidoglycan synthesis proteins. The changes in DivIVA expression can change the cells into sphere or “light bulb” shape [19,20]. Similar to the other microorganisms, FtsZ is a core component in cell division of *C. glutamicum*, aggregating in the middle of the cell to form a Z ring which causes the cell to divide. Inhibition of FtsZ expression let the whole cell get longer [21].

In this paper, we for the first time proposed a new idea that to enhance HA synthesis in the engineered *C. glutamicum* via cell morphology engineering. Through up- or down-regulating the expression levels of *divIVA* gene and *ftsZ* gene, respectively, the cell morphology of *C. glutamicum* was successfully changed and the cell volume was enlarged. And further, the effects of cell morphology changes on HA synthesis capacity and HAS expression of single cell was investigated.

2. Material and methods

2.1. DNA manipulation

DNA electrophoresis, Gibson assembly reaction, DNA enzyme digestion and ligation, and plasmids transformation were performed in accordance with the standard laboratory protocols. Phanta high-fidelity DNA polymerase (Vazyme, Biotech Co., Ltd., China) was used in PCRs (Polymerase Chain Reaction). Plasmid extraction kit, gel extraction kit and total bacterial RNA extraction kit were purchased from Omega Biotek (Norcross, GA, United States). Gibson assembly reaction kits were purchased from Clonesmarter Technologies (Scottsdale, AZ, United States). QuickCut restriction enzymes were purchased from Takara (Dalian, China). The reverse transcription kit and qRT-PCR master mix were purchased from Vazyme (China).

2.2. Plasmids and strain construction

The plasmids and strains used in this study are listed in Table 1. The primers used for gene amplifications are listed in Table S1. Plasmid pEC-Ptac was served as the backbone for *divIVA* gene and *ftsZ* gene. Plasmid pk18mobsacB with sacB which produced levansucrase was used to edit genome via double crossover homologous recombination.

2.3. Shake flask culture of recombinant C. glutamicum

The seeds of different engineered *C. glutamicum* were all cultured overnight at 30 °C with 50 μg/mL kanamycin in the LBG20 medium (NaCl: 10 g/L, yeast extract: 5 g/L, peptone: 10 g/L, glucose: 20 g/L).

When OD_{600} of the seed broth reached 2.5, it was added into 50 mL of fermentation medium with 2.5%v/v inoculum in 300 mL flask. The fermentation medium contained: corn syrup powder: 20 g/L, glucose: 40 g/L, $(NH_4)_2SO_4$: 30 g/L, KH_2PO_4: 1 g/L, K_2HPO_4: 0.5 g/L, $MnSO_4{\cdot}7H_2O$: 10 mg/L, $FeSO_4{\cdot}7H_2O$: 10 mg/L, and kanamycin, 50 μg/mL. After 3 h culture at 28 °C, 1 mM isopropyl-β-D-thiogalactoside (IPTG) was supplemented to induce the HAS expression and HA biosynthesis.

2.4. HA titer and HA average molecular weight determination

1 mL of fermentation broth was treated with 3 mL of ethanol and placed at 4 °C for 2 h. The supernatant was discarded by centrifugation (room temperature, 10000 rpm, 3min). The precipitate was dried at room temperature for 1 h and dissolved with 1 mL of deionized water. Then the HA titer in the supernatant obtained after centrifugation (room temperature, 10000 rpm, 3min) was measured by the modified CTAB method, as previously described [13,22].

Gel filtration chromatography (GFC) combined with a differential refraction detector was used to measure the weight-average molecular weight (Mw) of the HA. The details were reported previously as well [13,22].

2.5. RNA isolation, reverse transcriptase PCR, quantitative real-time PCR (qRT-PCR) assay

RNA isolation, reverse transcriptase PCR and qRT-PCR were performed as illustrated in our previous study [13]. The housekeeping gene was *dnaE* to normalize the target gene expression by using dnaE (qRT)-s/dnaE (qRT)-as. The target genes *divIVA* and *ftsZ* were analyzed by divIVA (qRT)-s/divIVA (qRT)-as and ftsZ (qRT)-s/ftsZ (qRT)-as, respectively.

2.6. Plate counting method and the fluorescence determined by flow cytometry

After measuring OD600, the fermentation broth was serially diluted 10^4, 10^5, 10^6 and 10^7 times with sterile water. Three LB plates were inoculated each with 0.2 ml dilutions of various concentrations and cultured overnight at 37 °C in incubator. Visible colonies were counted at 48 h. The diluted multiple of the plates which the number of single colonies between 100 and 500 were recorded. The relationship between OD600 and cell numbers was also calculated by diluted multiple and colonies.

The fermentation broths were diluted to 10^6 cells/mL with deionized water, and the fluorescence value of single cell was determined by flow cytometer S3e™(bio-rad) with the mCherry (RFP) channel. The bacterial solution without fluorescent gene was used as the negative control. The number and intensity of cells with fluorescence value greater than 10^2 were counted, and the fluorescence value of single cell was analyzed.

2.7. The cell morphology observed by optical microscope and TEM

2 μL fermentation broth was smeared on a glass slide. After heat-fixing of the cells over an alcohol burner flame for 10 s, the slide was stained in 0.1% fuchsin dye for 1 min, washed with the distilled water for 1 min, air-dried. Dropping 20 μL pine tar on the dyed cell, the cell morphology was directly observed with 100 × objective lens by NIKON Eclipse 50i.

TEM images of cell morphology at 48 h were gotten by HITACHI

Table 1
Plasmids and strains used in current study.

Plasmids and strains	Description	References
Plasmid		
pEC-P_{tac}	*rep* from native plasmid pGA1(GenBank: X90817.2) of *C. glutamicum*, $Kana^r$, P_{tac}, *lacI*	This work
pk18mobsacB	$Kana^r$, *sacB*, P_{lac}	[13]
pCas9-mcherry	RFP:Cas9, Amp^r	[37]
P_{lac}-DivIVA (part)	P_{lac}-DivIVA (part), $Kana^r$	This work
P_{lac}-FtsZ (part)	P_{lac}-FtsZ (part), $Kana^r$	This work
pX-AB	*rep* from pBL1, Cm^r, P_{tac}-*hasA-hasB-Ter*	[22]
pEC-AB	pEC-P_{tac} derivate, P_{tac}-*hasA-hasB-Ter*	This work
pEC-DivIVA	pEC-P_{tac} derivate, P_{tac}-*divIVA-Ter*	This work
pEC-FtsZ	pEC-P_{tac} derivate, P_{tac}-*ftsZ-Ter*	This work
pEC-AB-DivIVA	pEC-P_{tac} derivate, P_{tac}-*hasA-hasB-divIVA-Ter*	This work
pEC-AB-FtsZ	pEC-P_{tac} derivate, P_{tac}-*hasA-hasB-ftsZ-Ter*	This work
pEC-RFP:AB	pEC-P_{tac} derivate, P_{tac}-rfp:*hasA-hasB-Ter*	This work
pEC-RFP:AB-FtsZ	pEC-P_{tac} derivate, P_{tac}-rfp:*hasA-hasB-ftsZ-Ter*	This work
Strain		
E.coli TOP10	F-mcrAΔ(*mrr-hsdRMS-mcrBC*) ϕ80 *lacZ* ΔM15 Δ*lac* X74 *recA1 deoR araD139* Δ(*ara-leu*) *7697 galU galK rpsl* (*strR*) *endA1 nupG*	Solarbio
C. glutamicum ATCC13032	Wild type	[22]
C. glutamicum-P_{divIVA}: P_{lac}	Wild type derivate, P_{divIVA} replaced by P_{lac}, $Kana^r$	This work
C. glutamicum-P_{ftsZ}: P_{lac}	Wild type derivate, P_{ftsZ} replaced by P_{lac}, $Kana^r$	This work
C. glutamicum/pX-AB	Wild type derivate, pX-AB, Cm^r	[22]
C. glutamicum-P_{divIVA}: P_{lac}/pX-AB	*C. glutamicum*-P_{divIVA}: P_{lac} derivate, pX-AB, $Kana^r$, Cm^r	This work
C. glutamicum-P_{ftsZ}: P_{lac}/pX-AB	*C. glutamicum*-P_{ftsZ}: P_{lac} derivate, pX-AB, $Kana^r$, Cm^r	This work
C. glutamicum/pEC-DivIVA	Wild type derivate, pEC-DivIVA, $Kana^r$	This work
C. glutamicum/pEC-FtsZ	Wild type derivate, pEC-FtsZ, $Kana^r$	This work
C. glutamicum/pEC-AB	Wild type derivate, pEC-AB, $Kana^r$	This work
C. glutamicum/pEC-AB-DivIVA	Wild type derivate, pEC-AB-DivIVA, $Kana^r$	This work
C. glutamicum/pEC-AB-FtsZ	Wild type derivate, pEC-AB-FtsZ, $Kana^r$	This work
C. glutamicum/pEC-RFP:AB	Wild type derivate, pEC-RFP:AB, $Kana^r$	This work
C. glutamicum/pEC-RFP:AB-FtsZ	Wild type derivate, pEC-RFP:AB-FtsZ, $Kana^r$	This work

TEM(H–7650B) in the center of Biomedical Analysis, Tsinghua University.

3. Results

3.1. Down-and–up dual regulation strategies of FtsZ and DivIVA to obtain enlarged cells with enhanced surface-area

The most common way to change cell morphology is to regulate the expression of genes related to cell elongation and cell division, e.g. *divIVA* and *ftsZ*. As we know, DivIVA is an essential protein in *C. glutamicum* cell elongation. The oligomer-DivIVA proteins are located at the two poles of the cell, as scaffolds for the proteins which synthesizing peptidoglycan (as shown in Fig. 1a). Down/up dual regulation of DivIVA was both proposed to obtain sphere-like enlarged cells or "light-bulb" shape cells, respectively (Fig. 1b). When reducing the expression of DivIVA, the synthesis-direction of the cell wall will be no longer limited, thereby the cells can't maintain the short rod shape and become spheres. But when increasing the expression of DivIVA, it will be unevenly distributed at the two poles of the cell, resulting in higher synthesis rate of peptidoglycan on one side than the other, consequently forming the asymmetric "light-bulb" shapes. FtsZ is a core component in cell division of *C. glutamicum* and it is homologous to microtubulin in higher biological cells. The FtsZ proteins aggregate in the middle of the cell to form a Z-division ring, producing a contractile force that causes the cell to divide (Fig. 1a). Down-expression of FtsZ, that is, blocking the formation of cell division rings and forming conjoined multi-nucleated cells, is the regular idea to obtain elongated cells and thus obtain enhanced surface area of the cell membrane. On the contrary, we further proposed a new idea to obtain dumbbell-like enlarged cells through up-expression of FtsZ. In this design, the Z-ring will be over-produced, consequently disturbing the cell division and causing the long axis length of the *C. glutamicum* cells even longer (Fig. 1b). Since HA synthase is a kind of transmembrane enzyme, the enhanced cell volume means the enhanced surface area of individual cell and also the enhanced amount of HAS expression, consequently obtaining the enhanced capability of HA accumulation, as shown in Fig. 1c.

3.2. Construction of the morphology-regulated C. glutamicum recombinants

In *C. glutamicum* ATCC13032 host, the common promoter P_{lac} was weak compared with promoter P_{divIVA} and P_{ftsZ} [20,21]. To down-express the DivIVA and FtsZ, P_{lac} was thus selected to *in-situ* substitute the natural P_{divIVA} and P_{ftsZ}, respectively.

Suicide plasmid P_{lac}-DivIVA (part) and P_{lac}-FtsZ (part) with weak promoter P_{lac} and homologous arm of *divIVA* and *ftsZ* were both constructed, as shown in Fig. S1. After transforming into wild-type *C. glutamicum* ATCC13032, single crossover homologous recombination was occurred and the positive clones on kanamycin plate were selected. Colony PCR and gene sequencing results (as shown in Fig. S2) verified that two engineered strains: *C. glutamicum*-P_{divIVA}: P_{lac} and *C. glutamicum*-P_{ftsZ}: P_{lac}, with weakened promoter of *divIVA* and *ftsZ* in genome, were successfully obtained (as shown in Fig. 2a and b).

On the other hand, overexpression of *divIVA* and *ftsZ* was achieved by recombinant plasmids pEC-DivIVA and pEC-FtsZ with P_{tac} promoter and strong RBS sequences, as shown in Fig. 2c and d. Recombinant strain *C. glutamicum*/pEC-DivIVA and *C. glutamicum*/pEC-FtsZ over-expressing the DivIVA and FtsZ, respectively, was subsequently constructed after plasmid transformation.

3.3. Cell morphology changes of engineered C. glutamicum via down/up dual regulation of FtsZ and DivIVA

With the wild-type strain as control, the four morphometric-regulatory strains: *C. glutamicum*-P_{divIVA}: P_{lac}, *C. glutamicum*-P_{ftsZ}: P_{lac}, *C. glutamicum*/pEC-DivIVA and *C. glutamicum*/pEC-FtsZ, were cultured in flask for 48 in parallel. Cell samples at 24 h or 48 h were observed with both qRT-PCR (Fig. 3) and optical microscope (Fig. 4).

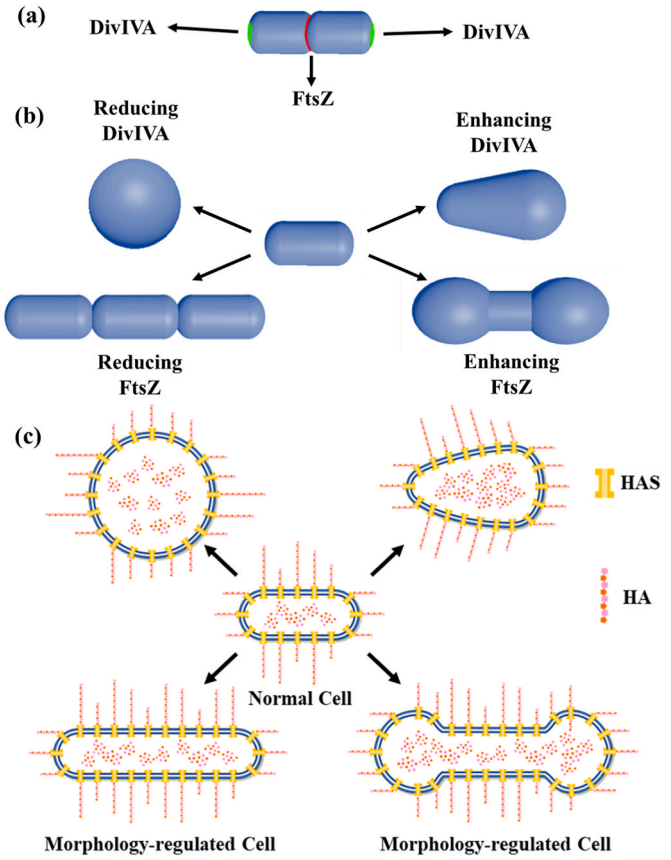

Fig. 1. Morphology engineering design of DivIVA and FtsZ to obtain enlarged cells with enhanced surface-area. (a) The locating positions of DivIVA and FtsZ in a cell. (b) Deduced morphology shifts of *C. glutamicum* after reducing or enhancing expression of DivIVA and FtsZ. (c) Morphology-regulated cells would improve the HAS expression and HA synthesis due to the enhanced surface-area.

As shown in Fig. 3, the results of qRT-PCR showed that the expression of *divIVA* gene and *ftsZ* gene was significantly reduced, only 0.12 and 0.42 of the wild gene, respectively, after P_{lac} substitution (Fig. 3).

As shown in Fig. 4, cells of the wild-type showed short rod shape under the optical microscope, with an axial length of 1.5 ± 0.2 μm and a radial length of 0.7 ± 0.1 μm. After reduced expression of *divIVA*, the cells obviously became spherical, with a diameter of 1.2 ± 0.2 μm. After enhanced expression of *divIVA*, however, the engineered cells looked like “light bulb” as deduced. The axial length increased to over 2.7 μm, and the radial length increased from 0.7 μm to over 1 μm.

For the *ftsZ* gene, the down or up expression regulation harvested even larger cell morphology changes. When expression of the *ftsZ* was reduced, the engineered cells were elongated and the axial length of some elongated cells reached 2.0 μm. When the *ftsZ* gene was overexpressed, the engineered cells were not only elongated, but also enlarged at two terminals, forming dumbbell-like engineered cells with the longest axial length even up to 7.0 μm (Fig. 4b).

According to the microscopic observed cells, we roughly estimated the length and diameter parameters of tens of cells for each strain, then roughly calculated the surface (membrane) area of a single cell before and after morphology changes, as summarized in Table 2 (The parameters and area formulas for various shapes were shown in Fig. S3). After morphological regulation, both reduced and enhanced expression of DivIVA and FtsZ increased the surface area of cell membrane. Relatively, up-regulation both showed remarkably larger cell surface area than down-regulation. For example, when overexpressing the *divIVA*, the membrane area of single cell was 2.9 folds of that of the original control; when overexpressing the *ftsZ*, it was even enhanced to 5.2 folds of the control.

3.4. HA biosynthesis with the morphology-changed C. glutamicum strains

Using the successfully constructed *C. glutamicum* strains with obvious morphology changes through down/up dual regulation of *divIVA* and *ftsZ* as hosts, we further introduced the biosynthetic genes of HA (*hasA* and *hasB*) via plasmid and enabled the novel engineered strains to produce HA. We had tested different clone strategies harboring different HA synthase genes, and finally we chose one *hasA* from *S. equi* subsp. *zooepidemicus* and one *hasB* form *C. glutamicum* as the superior biosynthetic genes [13].

Four engineered strains carrying down/up regulated *divIVA* and *ftsZ* in genome or plasmid, i.e. *C. glutamicum*-P_{divIVA}: P_{lac}/pX-AB, *C. glutamicum*/pEC-AB-DivIVA, *C. glutamicum*-P_{ftsZ}: P_{lac}/pX-AB and *C. glutamicum*/pEC-AB-FtsZ, were obtained (as shown in Fig. S4). Parallel cultures of the engineered strains were performed in flask with *C. glutamicum*/pX-AB without morphology regulation as control. Cell morphology, cell growth in term of the optical density (OD_{600}) and HA titer were observed or measured, as shown in Fig. 5.

When down-expressed the *divIVA* gene, the engineered cells still changed into small spherical in diameter 1.1–1.3 μm after introduction of the HA synthesis pathway; but when it was overexpressed, the morphology of the engineered cells only showed slightly difference from the control. And also, down-regulating the *divIVA* gene significantly inhibited the cell growth, resulting into very low cell biomass (the OD_{600} at 48 h decreased from 26.6 to 8.1) and thereby very low accumulated HA titer (< 2 g/L). On the contrary, up-regulating the *divIVA* didn't obviously affect the cell biomass and final HA titer (6.3 g/L), corresponding to the slight changes of their cell morphology.

The *ftsZ* dual regulation on HA production showed varied results. Down-expression of *ftsZ* gene significantly changed cell morphology into elongated cells as expected; but similar to *divIVA*-down regulation, cell growth was inhibited and thereby the final HA titer was significantly reduced. Interestingly, overexpression of the *ftsZ* gene remarkably enlarged the cells at even early 24 h (the axial length increased to 6–8 μm). The cell growth was again inhibited, but just slightly (OD600 reduced to 21.1 from 25.9); correspondingly, we harvested weakly reduced total HA titer (4.8 g/L).

We further calculated its HA synthesis amount of single cell through bacterial plate counting, and he results were summarized in Table 3. The average HA yield per cell was highly enhanced to 7.12 ng of *C. glutamicum*/pEC-AB-FtsZ from 0.49 ng of the control strain, which was as high as 13.5-fold increase.

3.5. Enhanced HAS expression on cell membrane contributes to the enhanced single cell HA synthesis capacity

For the FtsZ up-regulated strain, a red fluorescent protein RFP gene was further cloned and fused at the N-terminal of HAS gene (Fig. S5), to test if the HAS amount expressed on the membrane was enhanced due to the increase of the cell membrane surface area. The target RFP-positive strain *C. glutamicum*/pEC-RFP:AB-FtsZ and two control strains, *C. glutamicum*/pEC-RFP:AB (with RFP) and *C. glutamicum*/pEC-AB (without RFP), were cultured in parallel in flask, and the single cell fluorescence value of each strain was measured by flow cytometry, as shown in Fig. 6.

Compared with *C. glutamicum*/pEC-RFP:AB, the fluorescence intensity distribution of *C. glutamicum*/pEC-RFP:AB-FtsZ that overexpressed FtsZ shifted significantly to the right, and the average fluorescence intensity of a single cell increased from 431 units to 1345 units. This demonstrated that the FtsZ up-regulation did increase the HAS amount by 2.1 folds, accompanying with its enlarged cell size. That is, the overexpression of *ftsZ* gene successfully achieved higher HAS expression through larger cell size, consequently achieved higher

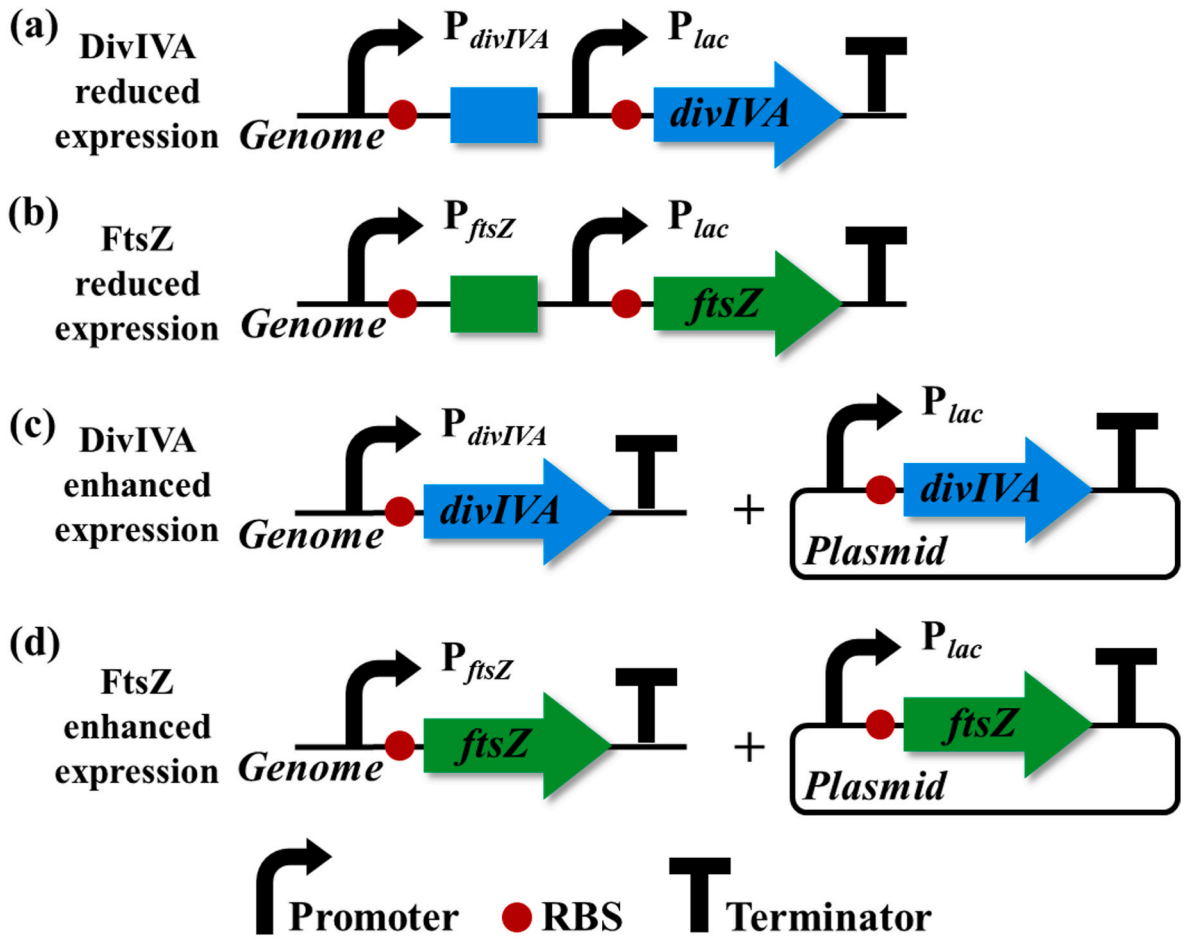

Fig. 2. Down or up expression strategies of *divIVA* and *ftsZ*. (a,b) Down-regulated strain: *C. glutamicum*-P_{divIVA}: P_{lac} and *C. glutamicum*-P_{ftsZ}: P_{lac}, respectively, constructed by in situ promoter replacement through single crossover homologous recombination. (c,d) Up-regulated strain: *C. glutamicum*/pEC-DivIVA and *C. glutamicum*/pEC-FtsZ, respectively, constructed by plasmids overexpression.

HA production capacity of a single engineered cell.

4. Discussion

Fundamental research on cell morphology regulation have been reported in many literatures. The change of cell morphology in eukaryotic cells is mostly based on the change of cytoskeleton. Microfilaments, microtubules and intermediate filaments are the components of cytoskeleton [23]. Most bacterial species have structural homologs of actin, tubulin and coiled coil filaments. The actins including MreB, FtsA, MamK, ParM and Alps, are assembled into helical or straight filaments in the bacterial cytoplasm. The essential cell division protein FtsZ forms a dynamic ring at mid-cell. It belongs to tubulins which also contain CetZ, TubZ and others [24]. And coiled coil filaments are more complex, for instance CreS, Scy, FilP, DivIVA, ESCRT-III and CrvA [25]. These proteins can all be used to regulate cell morphology. In *Escherichia coli*, *Bacillus subtilis*, and *Rhodobacter sphaeroides*, overexpression of MreB caused cells becoming larger [26–28]. In *E. coli*, *B. subtilis*, *Mycobacterium tuberculosis* and *C. glutamicum*, inhibition of FtsZ made the cells into long strips; while overexpression of FtsZ let the cells become dumbbell-shapes [21,28–30]. In addition to cytoskeleton related genes, we can also control each period of cell division by regulating cell cycle related genes, so as to obtain cells with different sizes and different specific surface areas as well [31,32].

But so far, only very few studies on enhancing the yield of target products by morphology engineering were reported. The most successful case was the production of PHA, a solid particle-like intracellular product. When morphological regulation made the volume of the single cell larger, the engineered cells could accommodate more

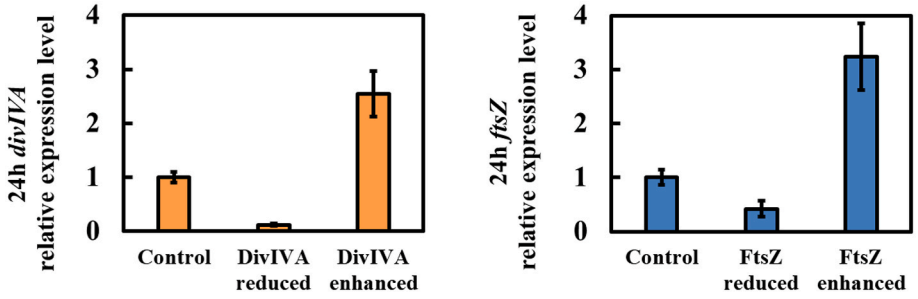

Fig. 3. Relative expression of *divIVA* and *ftsZ* in *C. glutamicum* after down/up-regulation of DivIVA and FtsZ with control strain (wild-type) by qRT-PCR. Relative expression levels were measured in triplicate at 24 h by qRT-PCR, and the error bars are the standard deviation. Control: wild-type; DivIVA reduced: *C. glutamicum*-P_{divIVA}: P_{lac}; DivIVA enhanced: *C. glutamicum*/pEC-DivIVA; FtsZ reduced: *C. glutamicum*-P_{ftsZ}: P_{lac}; FtsZ enhanced: *C. glutamicum*/pEC-FtsZ.

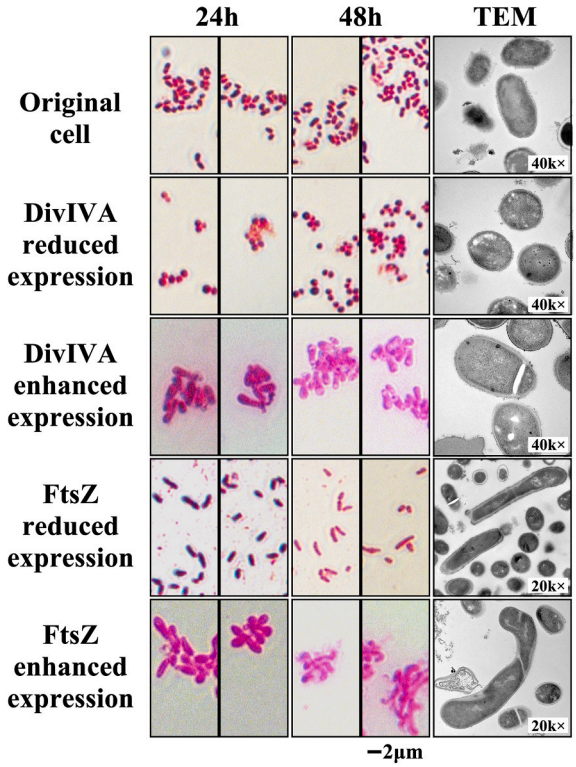

Fig. 4. Cell morphology changes of the *C. glutamicum* cells before and after down/up-regulation of DivIVA and FtsZ. Cell morphology were observed at 24 h/48 h by optical microscope, and at 48 h by TEM. Original cell: wild-type; DivIVA reduced expression: *C. glutamicum*-P_{divIVA}: P_{lac}; DivIVA enhanced expression: *C. glutamicum*/pEC-DivIVA; FtsZ reduced expression: *C. glutamicum*-P_{ftsZ}: P_{lac}; FtsZ enhanced expression: *C. glutamicum*/pEC-FtsZ.

PHA particles and thereby improve its productivity [4]. Besides, the poly-γ-glutamic acid (γ-PGA) titer of engineered *Bacillus amyloliquefaciens* was increased by 55.7% through MreB inhibition [33].

Unlike PHA, HA is a kind of extracellular products. That is, the cell volume is not a constraint limiting its yield. But HAS is a membrane-binding enzyme. Its expression amount on membrane is the key factor determining HA production capacity. Therefore, the larger surface area of cell (membrane) means the higher HAS expression capacity, thereby the higher HA titer probable. Based on this consideration, we proposed the novel idea in this work that regulating the cell size and membrane area to improve the HA production capacity of the single cell through cell morphological engineering.

Down-and-up dual regulation of both DivIVA and FtsZ in engineered *C. glutamicum* were proposed for the first time to change the morphology of cells. With respect to the down-regulation, up-regulation strategy was easier to achieve via plasmid expression. When DivIVA or FtsZ expression was up-regulated, bulb-shaped and dumbbell-shaped cells was formed, respectively. But surprisingly, after the introduction of HA synthesis pathway, the morphology of the engineered cells changed for the similar DivIVA and FtsZ up-regulated cells. Instead of bulb-shape or dumbbell-shape, the engineered cells became “small ellipsoid " or “long rods”, respectively. Particularly, up-regulation of FtsZ significantly enlarged the cells even at 24 h; for example, the axial length of the engineered cells increased to 6–8 μm from original 1–2 μm, which is far more effective than that of DivIVA control.

Cell morphology changes greatly affected cell division, thus reduced the number of cells and correspondingly reduced the total HA titer, no matter up- or down-regulation of DivIVA and FtsZ. To improve the final HA titer, the contradiction between the enlarged cell surface area and the reduced cell density must be solved. In the study of PHA, Jiang et al. introduced a temperature-induced *mreB* gene into the *mreB*-knockout cells to precisely control the expression of MreB through temperature [1], thereby successfully removed the cell growth inhibition arising from MreB overexpression. Similar strategy can also be applied in this HA production system. FtsZ can be lately-induced for overexpression via diverse inducers, and also dynamic metabolic regulation. Dynamic metabolic regulation can use designed regulatory elements to correlate the growth of bacteria, intracellular metabolites, signal molecules and other factors that changed with fermentation time, or controllable fermentation conditions such as temperature and light, with the target regulatory response [34,35]. For example, acetic acid, succinic acid and other by-products will be increasing produced during the production of HA. These by-products can be designed as ribose switches for dynamic regulation [36] of cell morphology-related genes, which would enlarge the engineered cells as expected in one hand; and didn't significantly affect the cell division and biomass accumulation in the other hand, therefore minimize the impact of morphogenetic changes on HA production.

Excitingly, the single-cell HA production capability was remarkably enhanced due to the cell enlarging regulation from FtsZ overexpression, although it reduced the cell numbers. By overexpression of *ftsZ*, the cell membrane area of a single cell was increased to 5.2 folds of the control; meanwhile, the expression of HAS in the membrane increased by 2.1 folds; and finally, the amount of HA synthesis titer of single cell highly increased by 13.5 folds as well. We deduced that this significant enhancement is because that not only the cell membrane area, but also the precursor materials, energy and production machines for HA synthesis in a single cell factory are all increased accompanying with enlargement of the cell size. Thus we can say that up-regulation of FtsZ is the optimal strategy to further enhance HA yield in the near future, after removing the morphological-change-resulted cell growth inhibition.

Cell morphology engineering will be a powerful new technology for enhanced production of various valuable products in green biomanufacturing, with the fast development of synthetic biology.

5. Conclusions

Cell morphology regulation toward *C. glutamicum* was carried out to try to enlarge the engineered cells, increase the HAS expression on cell membrane and thereby improve the single-cell HA producing capacity. DivIVA, the cell-elongation-related peptidoglycan supporting protein, and FtsZ, the cell division related protein, were both selected as regulation targets. Down/up dual regulation was performed via weak

Table 2
The estimated single-cell membrane area of each recombinant strain.

Stain	Cell Shape	Length/(μm)	Diameter 1/(μm)	Diameter 2/(μm)	Surface area/(μm^2/cell)
wild-type	rod shape	1.5 ± 0.2	0.7 ± 0.1	–	3.9 ± 0.7
C. glutamicum-P_{divIVA}: P_{lac}	sphere	–	1.2 ± 0.2	–	4.6 ± 1.1
C. glutamicum/pEC-DivIVA	light bulb	2.7 ± 0.4	1.3 ± 0.2	0.9 ± 0.1	11.4 ± 2.8
C. glutamicum-P_{ftsZ}: P_{lac}	long-rod	2.0 ± 0.3	0.7 ± 0.1	–	5.0 ± 1.7
C. glutamicum/pEC-FtsZ	dumbbell	7.2 ± 1.2	1.2 ± 0.1	0.7 ± 0.1	20.2 ± 3.6

Note: The length and diameter parameters of single cell were estimated by microscopic observation. Tens of cells for each strain were observed and the mean value of the length and diameter was calculated. Different area formulas for various shapes were described in Fig. S3.

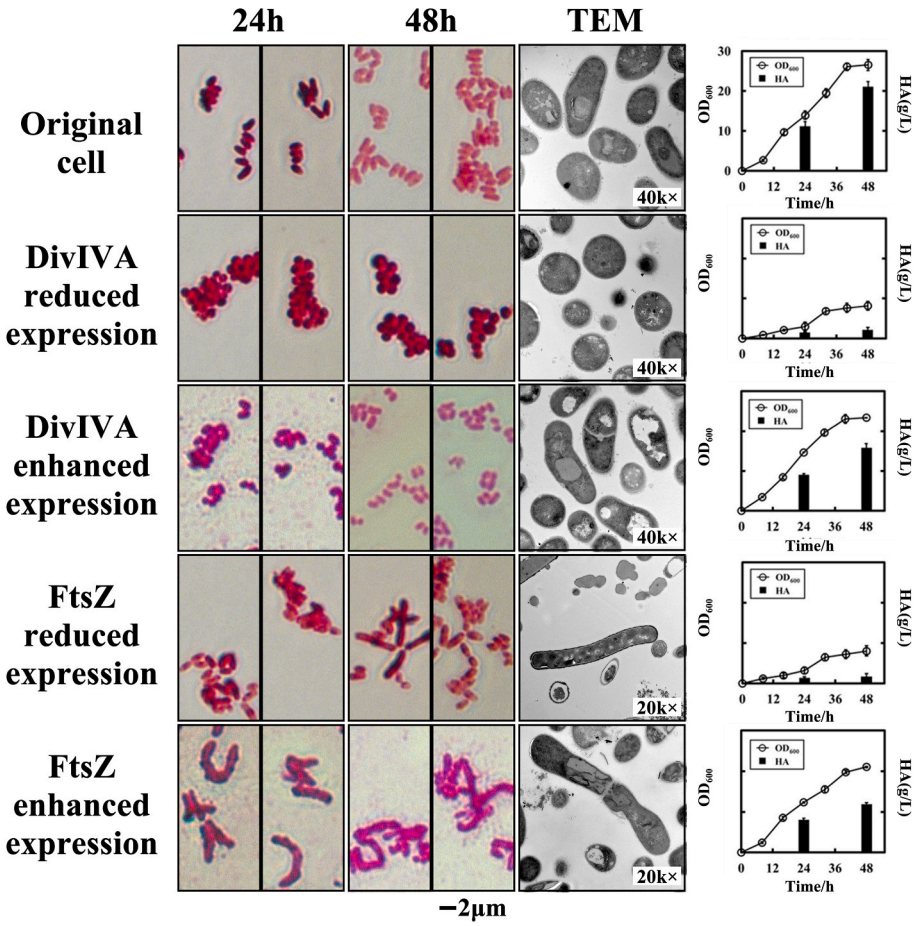

Fig. 5. Cell morphology and HA biosynthesis with the morphology-changed engineered *C. glutamicum* strains. Cell morphology were observed at 24 h/48 h by optical microscope, and at 48 h by TEM. OD600 were measured in triplicate from 8 h to 48 h. HA titers were measured in triplicate at 24 h and 48 h and the error bars are the standard deviation. Original cell: wild-type; DivIVA reduced expression: *C. glutamicum*-P_{divIVA}: P_{lac}/pX-AB; DivIVA enhanced expression: *C. glutamicum*/pEC-AB-DivIVA; FtsZ reduced expression: *C. glutamicum*-P_{ftsZ}: P_{lac}/pX-AB; FtsZ enhanced expression: *C. glutamicum*/pEC-AB-FtsZ.

promoter substitution or plasmid overexpression, respectively. Under non-HA synthesizing conditions, both reduced and enhanced expression of DivIVA and FtsZ significantly changed the cell morphologies of engineered *C. glutamicum* from natural short rod into morphology of small-ellipsoid-like (DivIVA-reduced), bulb-like (DivIVA-enhanced), long-rod (FtsZ-reduced) and dumbbell-like (FtsZ-enhanced), respectively. After HA synthesis pathway was introduced, only overexpression of FtsZ surprisingly changed the cell-shape into long and thick rod with 5.2-fold-increase of cell membrane area. Overexpression of FtsZ promoted the HAS expression on membrane significantly, which was verified by subsequent RFP fusion expression with HAS and flow cytometry analyses. Consequently, HA synthesis capability of the engineered *C. glutamicum* cells was immensely improved and we achieved 13.5-fold-increase of the single-cell HA producing yield.

In one word, FtsZ enhanced expression is the most optimal way to obtain the enlarged recombinant cells with slightly negative impacts on cell growth, thereby achieve the highest single-cell HA producing capacity. We can expect that the total HA productivity of the engineered cells will be further greatly enhanced after eliminating the influence of morphological regulation on cell growth, through optimizing the two-stage induction, introducing dynamic metabolic regulation and other synthetic biology new methods. Current work is also highly valuable for

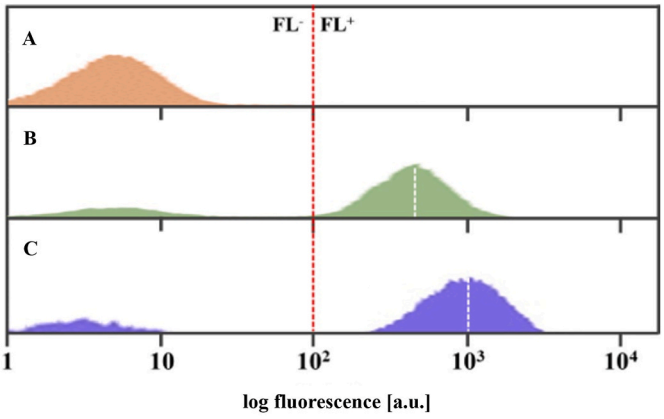

Fig. 6. HAS synthesis in single cell indirectly determined by flow cytometry. A: wild-type; B: *C. glutamicum*/pEC-RFP:AB; C: *C. glutamicum*/pEC-RFP:AB-FtsZ. The bacteria were cultured in the fermentation medium for 24 h, then diluted to 10^6/mL with deionized water for flow cytometry. The fluorescence less than 100 was considered as background. The abscissa represented the fluorescence value; the ordinate represented the number of cells. The white line represented the average fluorescence intensity.

Table 3
The number of cells corresponding to 1 OD_{600} and HA synthesis amount of single cell.

	The number of cells corresponding to $1OD_{600}$ (10^{10} cells/L)	HA synthesis amount of single cell (ng HA/cell)
C. glutamicum/pEC-AB	5.1 ± 0.9	0.49 ± 0.02
C. glutamicum/pEC-AB-FtsZ	0.32 ± 0.05	7.12 ± 0.18

other microbial products with similar limiting factors such as cell-volume and cell membrane.

Credit author statement

Conceptualization, Methodology, Investigation, Formal analysis, Writing - Original Draft, Writing - Review & Editing, Yukun Zheng; Conceptualization, Methodology, Investigation, Formal analysis, Writing - Original Draft, Fangyu Cheng; Investigation(part), Bo Zheng; Resources, Supervision, Project administration, Funding acquisition, Huimin Yu. All authors have read and agreed to the published version of manuscript.

Acknowledgement

This work was supported by National Key R&D Program of China [2018YFA0902200] and the National Natural Science Foundation of China [No. 21776157].

Appendix A. Supplementary data

Supplementary data to this article can be found online at https://doi.org/10.1016/j.synbio.2020.09.002.

References

[1] Jiang XR, Chen GQ. Morphology engineering of bacteria for bio-production. Biotechnol Adv 2016;34(4):435–40. https://doi.org/10.1016/j.biotechadv.2015.12.007.
[2] Wang Y. Engineering Escherichia coli for enhanced production of poly(3-hydroxybutyrate-co-4-hydroxybutyrate) in larger cellular space. Metab Eng 2014;25:183–93. https://doi.org/10.1016/j.ymben.2014.07.010.
[3] Daniel RA, Errington J. Control of cell morphogenesis in bacteria: two distinct ways to make a rod-shaped cell. Cell 2003;113(6):767–76. https://doi.org/10.1016/s0092-8674(03)00421-5.
[4] Jiang XR. Engineering the bacterial shapes for enhanced inclusion bodies accumulation. Metab Eng 2015;29:227–37. https://doi.org/10.1016/j.ymben.2015.03.017.
[5] Ye JW. Engineering of Halomonas bluephagenesis for low cost production of poly(3-hydroxybutyrate-co-4-hydroxybutyrate) from glucose. Metab Eng 2018;47:143–52. https://doi.org/10.1016/j.ymben.2018.03.013.
[6] Jiang D, Liang J, Noble PW. Hyaluronan in tissue injury and repair. Annu Rev Cell Dev Biol 2007;23:435–61.
[7] Blank LM, McLaughlin RL, Nielsen LK. Stable production of hyaluronic acid in Streptococcus zooepidemicus chemostats operated at high dilution rate. Biotechnol Bioeng 2005;90(6):685–93.
[8] Kendall FE, Heidelberger M, Dawson MH. A serologically inactive polysaccharide elaborated by mucoid strains of group A hemolytic streptococcus. J Biol Chem 1937;118(1):61–9.
[9] Im J-H. Optimization of medium components for high-molecular-weight hyaluronic acid production by Streptococcus sp. ID9102 via a statistical approach. J Ind Microbiol Biotechnol 2009;36(11):1337.
[10] Jin P. Production of specific-molecular-weight hyaluronan by metabolically engineered Bacillus subtilis 168. Metab Eng 2016;35:21–30.
[11] Mao Z, Shin H-D, Chen R. A recombinant E. coli bioprocess for hyaluronan synthesis. Appl Microbiol Biotechnol 2009;84(1):63.
[12] Sunguroğlu C. Higher titer hyaluronic acid production in recombinant Lactococcus lactis. Prep Biochem Biotechnol 2018;48(8):734–42.
[13] Cheng F. Enhanced biosynthesis of hyaluronic acid using engineered Corynebacterium glutamicum via metabolic pathway regulation. Biotechnol J 2017;12(10):1700191.
[14] Tatsumi N, Inui M. Corynebacterium glutamicum: biology and biotechnology. vol. 23. Springer Science & Business Media; 2012.
[15] Cheng F, Yu H, Stephanopoulos G. Engineering Corynebacterium glutamicum for high-titer biosynthesis of hyaluronic acid. Metab Eng 2019;55:276–89. https://doi.org/10.1016/j.ymben.2019.07.003.
[16] Wang Y. Eliminating the capsule-like layer to promote glucose uptake for hyaluronan production by engineered Corynebacterium glutamicum. Nat Commun 2020;11(1):3120. https://doi.org/10.1038/s41467-020-16962-7.
[17] Jacobs ML, Boyd MA, Kamat NP. Diblock copolymers enhance folding of a mechanosensitive membrane protein during cell-free expression. Proceedings of the national academy of sciences 2019;vol. 116(10):4031–6.
[18] Westbrook AW. Engineering of cell membrane to enhance heterologous production of hyaluronic acid in Bacillus subtilis. Biotechnol Bioeng 2018;115(1):216–31.
[19] Letek M. DivIVA is required for polar growth in the MreB-lacking rod-shaped actinomycete Corynebacterium glutamicum. J Bacteriol 2008;190(9):3283–92. https://doi.org/10.1128/jb.01934-07.
[20] Letek M. Cell growth and cell division in the rod-shaped actinomycete Corynebacterium glutamicum. Antonie Van Leeuwenhoek International Journal of General and Molecular Microbiology 2008;94(1):99–109. https://doi.org/10.1007/s10482-008-9224-4.
[21] Letek M. Characterization of the promoter region of ftsZ from Corynebacterium glutamicum and controlled overexpression of FtsZ. Int Microbiol 2007;10(4):271–82. https://doi.org/10.2436/20.1501.01.36.
[22] Cheng F. High-titer biosynthesis of hyaluronic acid by recombinant Corynebacterium glutamicum. Biotechnol J 2016;11(4):574–84.
[23] Fletcher DA, Mullins RD. Cell mechanics and the cytoskeleton. Nature 2010;463(7280):485–92.
[24] Vollmer W. The prokaryotic cytoskeleton: a putative target for inhibitors and antibiotics? Appl Microbiol Biotechnol 2006;73(1):37–47.
[25] Wagstaff J, Löwe J. Prokaryotic cytoskeletons: protein filaments organizing small cells. Nat Rev Microbiol 2018;16(4):187.
[26] Defeu Soufo HJ, Graumann PL. Bacillus subtilis MreB paralogues have different filament architectures and lead to shape remodelling of a heterologous cell system. Mol Microbiol 2010;78(5):1145–58.
[27] Slovak PM, Wadhams GH, Armitage JP. Localization of MreB in Rhodobacter sphaeroides under conditions causing changes in cell shape and membrane structure. J Bacteriol 2005;187(1):54–64.
[28] Tan Q, Awano N, Inouye M. YeeV is an Escherichia coli toxin that inhibits cell division by targeting the cytoskeleton proteins. *FtsZ and MreB.* Molecular microbiology 2011;79(1):109–18.
[29] Dziadek J. Physiological consequences associated with overproduction of Mycobacterium tuberculosis FtsZ in mycobacterial hosts. Microbiol 2002;148(4):961–71.
[30] Feucht A, Errington J. ftsZ mutations affecting cell division frequency, placement and morphology in Bacillus subtilis. Microbiol 2005;151(6):2053–64.
[31] Ding Q. Light-powered Escherichia coli cell division for chemical production. Nat Commun 2020;11(1):1–14.
[32] Zheng H. General quantitative relations linking cell growth and the cell cycle in Escherichia coli. Nat Microbiol 2020:1–7.
[33] Gao W. Effects of MreB paralogs on poly-γ-glutamic acid synthesis and cell morphology in Bacillus amyloliquefaciens. FEMS Microbiol Lett 2016;363(17).
[34] Chubukov V. Coordination of microbial metabolism. Nat Rev Microbiol 2014;12(5):327–40.
[35] Holtz WJ, Keasling JD. Engineering static and dynamic control of synthetic pathways. Cell 2010;140(1):19–23.
[36] Wu MJ. Automated design of diverse stand-alone riboswitches. ACS Synth Biol 2019;8(8):1838–46.
[37] Shaner NC. Improved monomeric red, orange and yellow fluorescent proteins derived from Discosoma sp. red fluorescent protein. Nat Biotechnol 2004;22(12):1567–72.